

# Metal Target Discrimination with a Commercial Two Frequency Sensor— Part I: Raw Data Analysis in the Complex Plane

Claudio Bruschini

École Polytechnique Fédérale de Lausanne – LAP  
EPFL–I&C–LAP, CH–1015 Lausanne, Switzerland  
Claudio.Bruschini@epfl.ch

Vrije Universiteit Brussel – ETRO-IRIS  
Pleinlaan 2, B-1050 Brussels, Belgium

## Abstract

We have analysed an extensive amount of metal detector raw data using a commercially available differential CW system, the Förster Minex 2FD, and will discuss in particular the target response variation in the complex plane for reference objects (cylinders), a *minimum-metal mine's* components, a PMN mine and *metallic mines*, and *metallic clutter pieces*. The detailed response analysis has allowed to highlight a number of effects such as orientation dependencies, changes due to axial offsets, variability in the response of composite objects, as well as fluctuations in the soil signal. We have also shown that it is possible to distinguish smaller clutter items from larger objects, and that *some mines* have quite *characteristic responses* (e.g. PMN). A “*qualitative*” (*coarse*) *target classification is therefore possible*, at least for situations with a sufficient signal to noise (S/N) ratio. Quantitative aspects are dealt with in a companion article [1].

## 1. Introduction

Frequency domain data has been acquired with a Förster Minex 2FD, a commercially available differential two-frequency continuous wave metal detector (MD) operating at 2.4 kHz ( $f_1$ ) and 19.2 kHz ( $f_2$ ) [2]. Linear scans, and in some cases series of parallel scans as well, have been carried out with a high density of points in the scan direction, placing the detector on a Cartesian gantry. First results have been detailed in [2].

The metal detector signals [2]–[3] we are looking at correspond to the real ( $f_1 0^\circ$ ,  $f_2 0^\circ$ ) and imaginary parts ( $f_1 90^\circ$ ,  $f_2 90^\circ$ ) (in the complex plane) of the analog signals  $V_1^{(s)}$  and  $V_2^{(s)}$  induced at  $f_1$  and  $f_2$  in the receiver. The induced voltages are in fact scaled [2]–[3] to effectively remove their linear dependency on the operating frequency  $\omega$ , which allows us to compare their ratios and trends with those of a target's theoretical response function.

## 1.1. Complex Plane Plots

We will make extensive use in the following of the *complex*, or impedance, *plane* representation, in which each measurement at  $f_1$  is represented as a point of coordinates ( $f_1 0^\circ, f_1 90^\circ$ ), and similarly for  $f_2$ . As the detector is displaced with respect to the target, these points move in a 2D plane along characteristic lines, which appear to be continuous in our case due to the high density of measurements. Each point's (phase) angle represents the phase shift of the induced voltage with respect to the transmitted one, at the given position.

Complex plane plots allow an intuitive, visual analysis of an object's phase and amplitude response behaviour, and help in target comparison. Because of the detector's differential nature they are in our case often symmetric with respect to the origin (positive and negative response). Indeed, the response increases and reaches a maximum as the detector approaches the target, goes to zero straight over it (plot's origin), reaches a minimum and goes back to zero as the detector moves away from the target.

In general the phase response decreases monotonically for increasing MD operating frequency, target size or conductivity, ranging from  $+90^\circ$  for a purely magnetic object (positive values are typical of ferromagnetic targets), to  $-90^\circ$  for a massive, conductive body. In practice open, irregular curves are often recorded: they are typical of ferromagnetic or composite objects and indicate important phase changes along the scan, whereas straight lines, characteristic of most non-ferromagnetic objects, imply a constant phase response, equal to the curve's slope.

Complex plane plots could also be obtained when manually scanning over the object by providing a start and stop signal and maintaining a constant scanning speed, although the results would obviously be less precise. Background signal subtraction could then be implemented as well, at least to first order, by filtering the data.

## 1.2. Background (soil) Signal Subtraction

Most of the scans have been carried out on objects placed on the surface (usually for small objects) or just underneath it (*flush*), to ease data acquisition while at the same time partly taking into account the response from the soil itself. The latter is not negligible, even under these conditions, when looking at some of the smaller objects. Background (soil) scans should therefore ideally be taken for each object in 1D (along a line) or 2D (parallel lines). As a practical compromise we decided to take background scans before and after each series of scans.

## 1.3. Definitions

In the standard scanning setup the metal detector (MD) is perfectly horizontal, and its axis is perpendicular to the scanning direction. The *Horizontal (HOR) Plane* is defined by the metal detector head (i.e. parallel to the ground surface) and is the plane into which the metal detector moves. Four main orientations with respect to the scanning direction are possible for a target object lying in the horizontal plane and with centre along the scanning direction, namely *PER* (perpendicular to the scanning direction), *PAR* (parallel), *QUI* (along the main diagonal) and *QU4* (at 90° to the main diagonal).

The *Vertical (VER) Plane* is defined by the metal detector support structure (Z: vertical axis) and the scanning direction. An object placed vertically is labelled “*VER*”.

## 2. Data Collection Results: Reference Objects

Before moving to more complex objects and scenarios it is useful to study the response of canonical targets, of size and composition similar to those of interest in landmine detection. We will detail in the following some of the results, in particular orientation effects, for *cylindrical objects* which will be labelled as *coc* (copper) and *msc* (mild steel). Two cylinder sizes were used, “large” (code: 2) and “small” (code: 1), with diameter 0.7 and 0.3 cm respectively, and 3 cm length in both cases. A small copper cylinder is labelled as *coc1*, a large one as *coc2*, etc. More complete results are detailed in [3].

*Comparison between Vertically/Horizontally placed objects (VER vs. PAR, PER orientations):*

- *Ferromagnetic object* (Figure 1): the shape of the *VER* curve is a straight line (like for *PER*), the phase is however closer to the one of *PAR*,

possibly because the contribution from the field along the cylinder axis is dominant (**orientation sensitivity of short ferromagnetic parts**).

- *Non-ferromagnetic object*: tests were carried out with the copper reference cylinders. In general **nearly identical phases are recorded for all orientations**. Similar results should hold for other non-ferromagnetic objects.

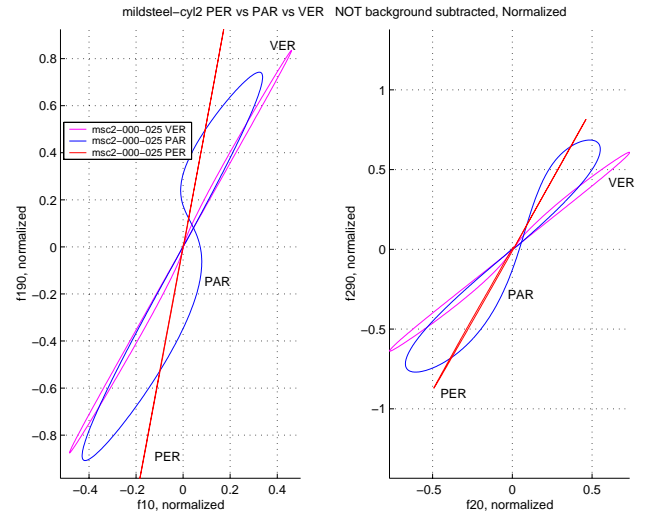


Figure 1: Response at  $f_1$  and  $f_2$  to a mild steel cylinder (*msc2*) for different orientations: *VER* vs. *PAR* vs. *PER*. Normalized.

## 3. Phase vs. Distance (depth)

Scans at increasing distance from the object were carried out raising the detector head in 1 or 2 cm increments, without displacing the object.

### 3.1. Ferromagnetic Cylinders in the Horiz. Plane

The response of a large ferromagnetic cylinder (*msc2*) for each of the four orientations in the *HORizontal plane* has been analysed at increasing detector heights [3], and is similar to the one for a small ferromagnetic cylinder (*msc1*) featured in Figure 2. *The PER profiles do not change, whereas the PAR ones do and become somewhat more irregular (larger variation in phase angles) with increasing height.* An exception is the straight section in each plot, which stays unchanged; it corresponds to the approach phase and when moving away from the object.

Similar comments apply for a small ferromagnetic cylinder (*msc1*, see Figure 2), with the various effects just illustrated being more marked than for *msc2*.

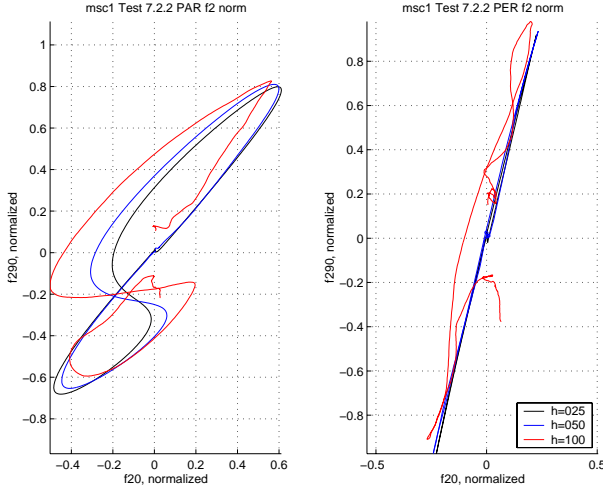


Figure 2: Response at  $f_2$  to a small **mild steel cylinder (msc1)** placed flush with the surface, **at increasing detector heights** (2.5, 5 and 10 cm) for the *PAR* and *PER* orientations in the horizontal plane. Normalized.

### 3.2. Target in Vertical Plane

Tests were carried out with a vertical reference copper cylinder (**coc2**). All scans at increasing heights featured nearly identical phases. Scans at different heights were also analysed with a vertical **msc2** cylinder, i.e. an elongated ferromagnetic object. The phase stays constant from one to the other. This is not true any more for parallel scans at a fixed height (see again §4). Similar effects for prolate steel spheroids at a fixed orientation have been reported using a time domain system in [4].

### 4. Phase vs. Axial Offsets (Parallel Scans)

The behaviour of scans not carried out exactly over the target has been analysed by means of series of parallel scans at constant detector height and object position. Results will be shown in this paragraph for some reference cylinders. Results for other objects (minimum-metal mine, **PMN** mine) are detailed in §8 as well as in [3].

#### Ferromagnetic Object in the Vertical Plane

The response of a ferromagnetic cylinder (**msc2**) placed *vertically* is analysed in Figure 3 (normalized) when approaching the object: the phase clearly *decreases*, i.e. moves towards  $0^\circ$  (there is a *clockwise curve rotation* when moving from scan 5 to 9). All curves are slightly open (not straight lines); this situation bears similarity to what shown in Figure 1 (*VER* vs. *PER* orientations). The

phase is on the other hand constant for parallel scans passing over target (not shown).

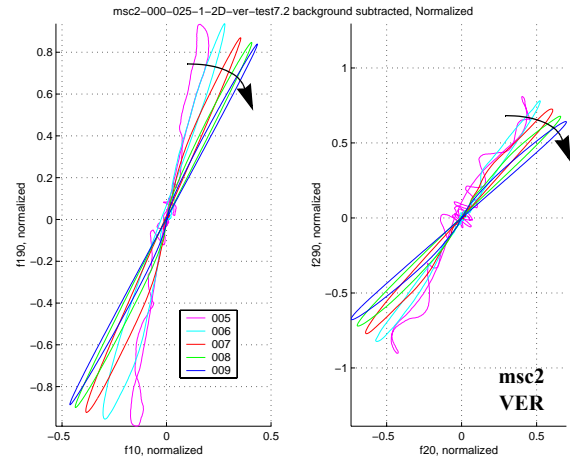


Figure 3: 2D response (parallel scans) at  $f_1$  and  $f_2$  to a **mild steel cylinder (msc2)** placed **vertically** (top at surface level); normalized, scans 5-9 (approach phase). Scan separation: 2 cm.

## 5. Phase vs. Orientation in the Horizontal Plane

### Non-ferromagnetic Cylinders

**Non-ferromagnetic cylinders**, e.g. of aluminium or copper, **do not show any noticeable difference** (see also previous discussion for **coc2** in §2).

### Ferromagnetic Cylinders

The non-normalized response of a ferromagnetic cylinder (**msc2**) is shown in Figure 4 at fixed heights for each of the four orientations in the **HORizontal** plane. **The response is strongly orientation dependent.** At  $f_1$  the *PAR* orientation features the largest amplitude, *PER* the smallest. The *PAR* profile is “figure 8” shaped, *PER* linear, *QU1* and *QU4* intermediate. The behaviour at  $f_2$  is similar, but the “figure 8” curves are more regularly shaped (symmetric).

The curves for the smaller cylinder (**msc1**) show similar trends, with an even more marked difference between the *PAR* and *PER* configurations.

## 6. Summary of Orientation/Distance Effects

We can summarise the most important results concerning orientation and distance effects as follows:

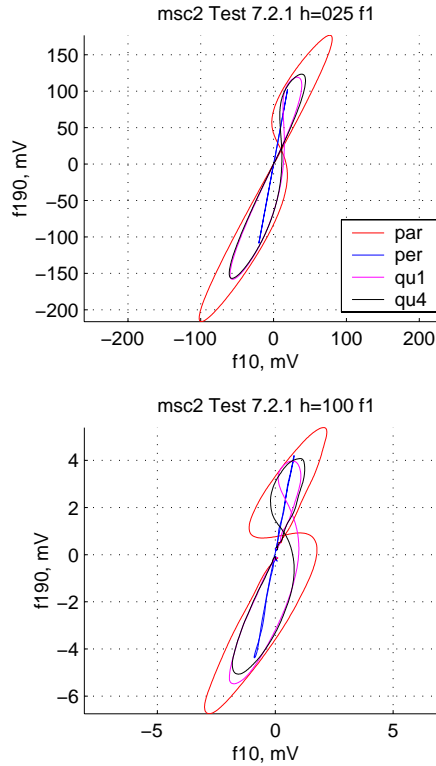


Figure 4: Response at  $f_1$  to a mild steel cylinder (**msc2**) placed flush with the surface, at fixed heights (2.5 and 10 cm) for each of the four orientations in the horizontal plane.

- The response of **non-ferromagnetic objects** is usually not strongly orientation sensitive, nor influenced by height (distance) variations or axial offsets; exceptions are possible, e.g. for large objects close to the detector.
- The response of (elongated) **ferromagnetic objects** is usually strongly *orientation* dependent, all the more so for those configurations in which the primary magnetic field moves from being predominantly aligned along the symmetry axis to being predominantly perpendicular to it, or vice versa.
- The response of (elongated) **ferromagnetic objects** can therefore also change considerably with the detector *distance*, depending on their orientation.

## 7. Minimum-metal Mine and its Components

We will analyse in the following the response of an L111 minimum-metal mine and of its components. Although this particular type of mine is not widely diffused, it is still

representative of the category, and will allow to draw a number of interesting conclusions.

### 7.1. Comparison of Striker Pins

*Different versions of the L111 striker pin have been compared among them and with the striker of a real mine tested at the EPFL. No differences were detected.*

Measurements were also carried out with the striker pin in the horizontal plane, parallel (*PAR*) and perpendicular (*PER*) to the scanning direction. This corresponds to an *unusual placement of the mine*, which however can not be totally excluded a priori, either due to natural events or to a deliberate act. The resulting behaviour is quite similar to what previously described for the larger steel cylinder (**msc2**) in §2 (see Figure 1), *with in particular an important difference between the VER and PER orientations*. The signal amplitudes decrease in the following order: *VER*, *PAR*, *PER* (barely detected at the medium MD sensitivity setting). The target's detectability depends therefore here strongly on its orientation.

The overall mine response would obviously include the contribution from the detonator as well.

### 7.2. Comparison of Mine Detonators

*Comparison with real detonator:* A replica detonator (**mid**) (essentially composed of a cylindrical foil), provided by the Swiss Defence Procurement Agency, was compared to the original detonator of the real mine tested at the EPFL (**midereal**). *The behaviour is similar but the phases are not identical* (Figure 5); the replica detonator does therefore represent a good but not perfect reproduction. The actual phase angle at  $f_1$ , which is quite small, is in fact slightly lower than what shown due to important background effects. Also, the response at  $f_1$  is much weaker than at  $f_2$ , characteristic of a quite small and/or poorly conductive non-ferromagnetic object.

*Comparison at different heights:* The response *does not change* at least up to 10 cm, although it is quite weak at  $f_1$ . At 15 cm the target is barely detectable at the maximum sensitivity setting.

*Comparison of different orientations (VER vs PER, PAR):* no changes in phase response are apparent.

### 7.3. “Upside down” Mine

A complete mine was placed “upside down”, i.e. with the striker above the detonator, as well as on its side. The response is quite different from the standard one, the

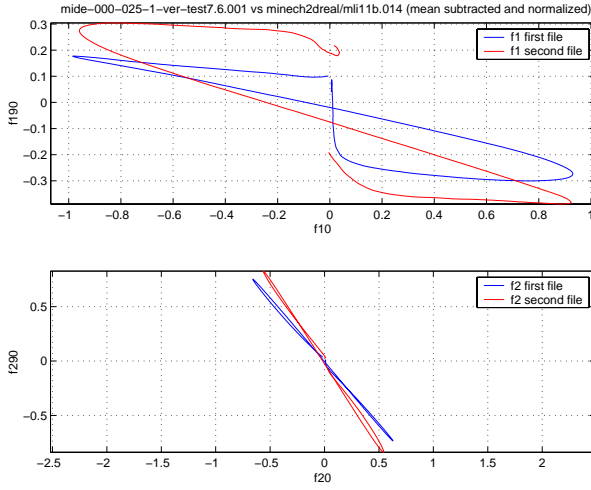


Figure 5: Minimum-metal mine detonators: replica (**mide**) vs. original one (**midereal**); normalized.

striker pin prevailing in the first case (closer to the coil). This is a good example of a target discrimination problem due to the behaviour of composite objects.

## 8. Response for a PMN mine

We will analyse in the following the response of the Russian PMN, a widely diffused non minimum-metal AP mine.

### 8.1. Phase vs. Distance (depth)

PMN data was collected at the VUB sandbox with the mine at different depths (5, 10, 20, 26 cm to top of mine). The PMN used in these tests (**pmnVUB**) featured the ferromagnetic cover retaining ring; it was not yet armed. We concentrated on background subtracted data to obtain the response from the mine alone. **Some phase response differences with depth were clearly visible** [3]. In addition the phase response at  $f_1$  is strongly dependent on the position along the scan.

### 8.2. Phase vs. Axial Offsets (parallel scans)

Four different orientations were analysed in the horizontal plane, namely *PAR1* followed by 3 successive counter clockwise rotations: *PER1*, *PAR2* and *PER2*. Thirteen 2D scans were carried out at a pitch of 4 cm.

The data corresponding to the *PAR1* configuration is shown in Figure 6, top. The target looks typically ferromagnetic at large distances (scan 3 for example); the response “rotates” then towards the response above the

target, scan 7. The latter seems clearly non-ferromagnetic at  $f_2$  (eddy current effects prevail), a superposition at  $f_1$ .

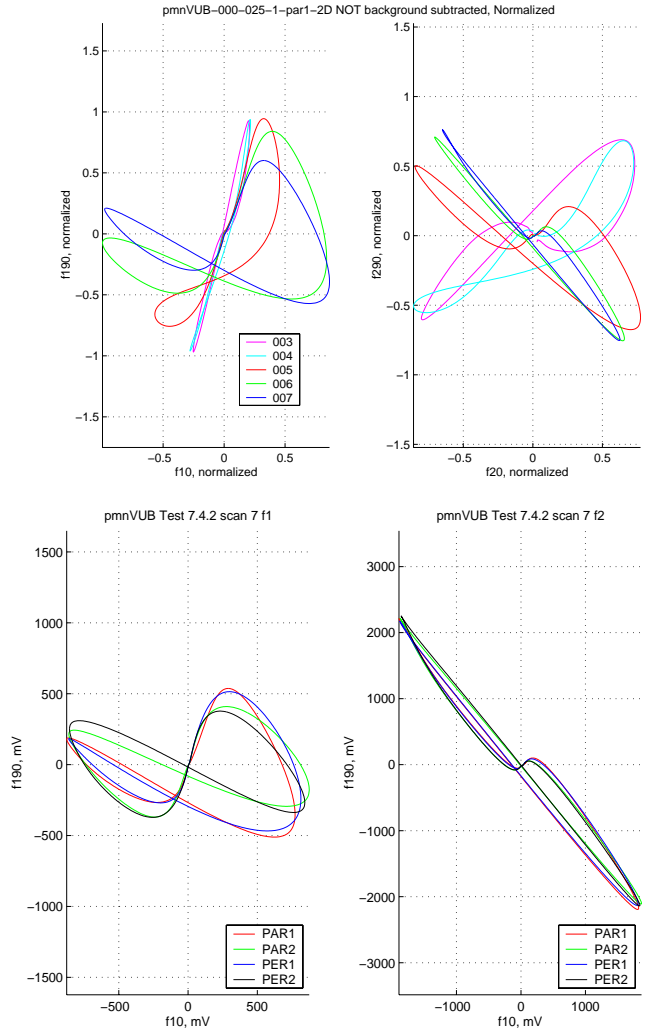


Figure 6: *Top half*: 2D response (**parallel scans**) at  $f_1$  and  $f_2$  for **pmnVUB**, placed at *PAR1* (HOR plane). Normalized, scans 3-7 (approaching the target; centre of target between scans 7 and 8), 4 cm distance between scans. *Bottom half*: Comparison of the response at  $f_1$  and  $f_2$  over **pmnVUB**, for 4 orientations in the HOR plane; scan 7 (above the target).

**Very important phase response differences with axial offset are clearly visible.**

### 8.3. Different Orientations in the Horizontal Plane

*PAR1* and *PER1*, *PAR2* and *PER2*, are similar although not identical as clearly shown in Figure 6, bottom, in particular far from the object (approaching and moving away). **Phase response differences with target**

**orientation in the horizontal plane are therefore apparent.** Also, the amplitude of the response at  $f_2$  is much larger than at  $f_1$ .

Summarising, the response of a **PMN** represents a good example of a composite object whose phase response can vary considerably with axial offset and orientation (open curves at  $f_1$ , etc.) and is **quite typical**.

## 9. Response for Metallic Mines and (composite) UXO

Metallic AP mines, such as *bounding fragmentation* and *stake fragmentation mines*, are usually designed to kill via fragmentation, up to some tens of meters, and are composed of a relevant mass of metal as well as of explosive. The first are designed to be buried, the second to be placed on a (wooden) stake just above the surface.

Metallic mines are in principle easier to detect, often even visually. There are however circumstances in which the stake mine is found lying on the surface, in case the wooden stake breaks or rots for example, or even buried. In addition, *if we are relying on a discriminative metal detector we must be sure that the signal from such a type of mine is not going to be rejected by error.* We have therefore investigated the response of the previously mentioned mines, as reported below.

### 9.1. PROM – Bounding Fragmentation Mine

A cylindrically shaped **PROM** bounding fragmentation mine, whose steel body is about 20 cm long, was buried vertically, with only the top (a pronged striker about 4 cm long) sticking above the soil, and acquisitions taken in 2D. The results are shown in Figure 7, top.

The target is so massive that the phase angle at  $f_1$  has turned from clearly positive to quite close to  $0^\circ$  (compare with the case of the smaller **PMR-2A** mine discussed below). Additional information is therefore necessary in this case to avoid mistaking the mine for a (small) non-ferromagnetic object. Incidentally, the overall amplitudes are not very large in this case, given the mass of the mine, and they change only slightly over it. Relying on target amplitude alone to discriminate such an object can therefore be dangerous.

### 9.2. PMR-2A – Stake Fragmentation Mine

*Vertical orientation:* A cylindrically shaped **PMR-2A** stake fragmentation mine, also made of steel and overall

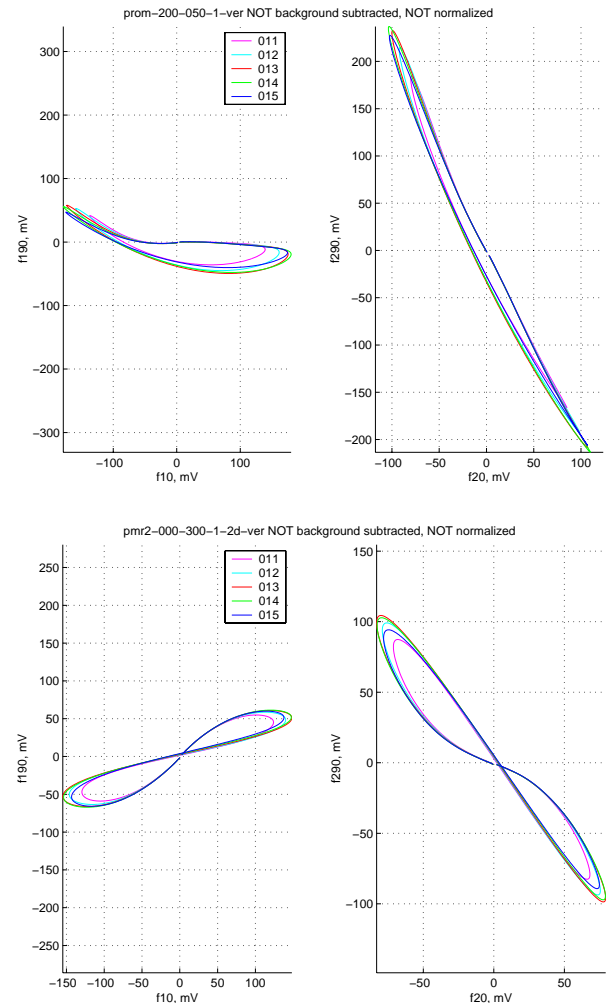


Figure 7: 2D response (parallel scans) at  $f_1$  and  $f_2$  to: *Top half:* a **PROM** mine placed **vertically** (pronged striker above surface); *Bottom half:* a **PMR-2A** mine placed **vertically** (mine above surface). Scans 11-15 (passing over the target). Distance between scans: 2 cm.

about 20 cm long, was placed vertically above the ground, and acquisitions taken in 2D. The results, shown in Figure 7, bottom, represent a **nice example of the response of a large ferromagnetic object**, with a positive phase response at  $f_1$  and a largely negative one at  $f_2$ , with open curves (typical of ferromagnetic objects), and *would allow an easy target identification*.

*Perpendicular and Parallel orientation:* Measurements were also carried out with a mine lying on the surface, as if it had fallen down. The phase response is rotated at both frequencies towards the vertical compared to the *VER* configuration; it is however still positive at  $f_1$  and negative at  $f_2$ , like in Figure 7, bottom, with quite a large phase difference between the two values, and *should therefore*



still be quite distinctive. This situation bears some similarity to the results for the large reference cylinder (**msc2**), *VER* vs. *PER* configurations (see Figure 1).

### 9.3. A Composite UXO Example

Tests were also carried out with a 20 mm projectile, an interesting **composite object** about 14 cm long, featuring a non-ferromagnetic tip (likely aluminium) on top of a cylindrical steel body. The overall response can therefore be **highly orientation-dependent**, according to the strength of the responses of the two parts. In spite of this, the target can be clearly identified at all orientations as a large (mostly) ferromagnetic object.

Summarising, the response of some **metallic mines** and UXO (Unexploded Ordnance) can in part be well approximated by the response of **large ferromagnetic cylinders**, which typically have a positive phase at  $f_1$  and a negative at  $f_2$ , as nicely shown by the quite characteristic response of a **PMR-2A** mine, or even both negative such as for a **PROM** mine. The latter could be mistaken for a non-ferromagnetic object discriminating on the phase response alone.

## 10. Clutter (Debris) Analysis

During tests carried out by the EPFL DeTeC team in Cambodia with a GPR prototype, numerous metallic debris samples were collected from a simulated minefield situated next to a village. The end user team (Halo Trust) followed its standard operating procedures using an Ebinger Ebex 420 SI MD. Each metallic piece, or set of pieces, was then removed and collected; the collected clutter should therefore be representative. Examples of results will be shown in the following for groups of similar objects; complete results are detailed in [3].

### 10.1. Debris Group #1 – cylindrical ferromagnetic

Objects in this group are mainly ferromagnetic and cylindrical, such as nails, of length ranging from 2.5 to 6 cm and diameter of 0.2 to 0.6 cm. MD signals for the *PAR* orientation (Figure 8) are usually quite stronger than for *PER*. The responses are similar to those of the ferromagnetic reference cylinders previously discussed.

### 10.2. Debris Group #2 – non-ferromagnetic foils

Objects in this group are **non-ferromagnetic foils** of

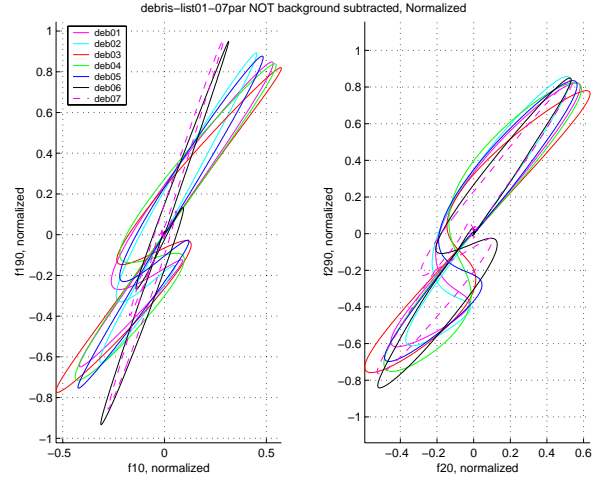


Figure 8: Response at  $f_1$  and  $f_2$  to cylindrical ferromagnetic debris (**deb01-07**) in the horizontal plane, *PAR* orientation; normalized, objects on the surface.

irregular shape, with sides ranging from about 1 to 10 cm. Their main characteristics are a mostly quite weak response, especially at  $f_1$ , with all phases close to  $0^\circ$ , excepted **deb20** (Figure 9, left). Plotting the phase difference would give a very low value for all objects (excepted **deb20**), resulting in good discrimination [1].

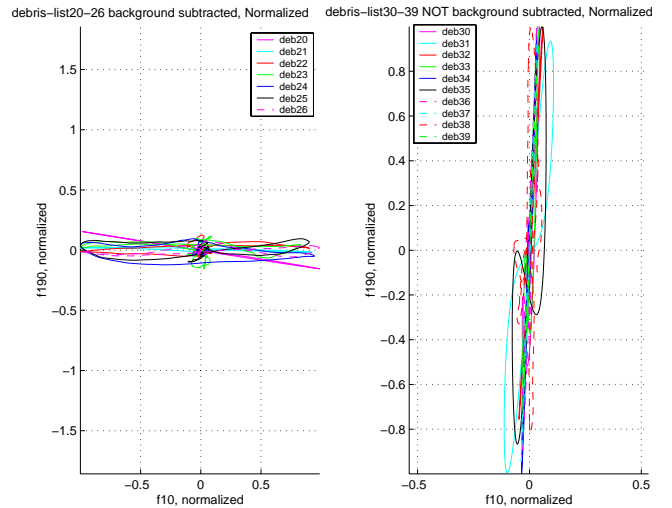


Figure 9: Response at  $f_1$  to non-ferromagnetic foils (**deb20-26**, left half) and ferromagnetic foils (**deb30-39**, right half) in the horizontal plane; normalized, objects on surface.

### 10.3. Debris Group #3 – ferromag. foils/fragments

Objects in this group are **ferromagnetic foils** and collections of **small fragments** thereof, of irregular shape, with sides ranging from about 1 to 5-6 cm. Their phase

responses (Figure 9, right) are mostly quite close to  $+90^\circ$ . Some of them give small phase differences, and sometimes, when the amplitudes at  $f_1$  and  $f_2$  are quite close, small amplitude difference values as well. This could again be used as a discrimination criterion.

Summarising, several tens **metallic clutter pieces**, mostly collected in Cambodia on a simulated mine field, have been analysed. Most of the clutter seems to be *ferromagnetic*.

- **Small ferromagnetic pieces** (nails, plates, pieces) feature mostly a phase response between  $+90^\circ$  and  $+45^\circ$  (indicative values), foils even less, between  $+90^\circ$  and about  $+75^\circ$ .
- **Non-ferromagnetic foils** feature mostly a small phase response, between  $0^\circ$  and about  $-15^\circ$ .
- **These clutter items can be quite clearly distinguished from the response of larger objects** (at least under laboratory conditions) and could constitute a basis for object discrimination. Larger clutter items are harder to discriminate, although this could still be possible when looking for mines with larger metallic components.
- Some ferromagnetic objects have quite an irregular response, e.g. a bottle cap, and are correspondingly harder to discriminate.

## 11. Conclusions

In this article we have dealt mostly with **qualitative** aspects of a metal detector's **phase response** to targets of interest in humanitarian demining applications, looking at signal trajectories in the **complex plane**. This method, inspired from NdT, makes it possible to exploit global object properties rather than only local ones. Similar work has also been carried out independently by Szyngiera [6].

*A number of theoretical elements of the basic models for the response of spheres and cylinders have been confirmed*, as detailed in [3]. *Fluctuations in the soil signal* are also clearly documented in the experimental data, which affect in particular the identification of small and/or deep objects; similar conclusions have been reached using the GEM-3 sensor [5].

The detailed response analysis has also allowed to highlight a number of effects such as orientation dependencies or changes due to axial offsets (elongated ferromagnetic targets), or subtle effects such as the response of composite objects and their variability.

We have also shown that it is possible to distinguish smaller clutter items from larger objects, and that *some mines* have quite *characteristic responses* (e.g. **PMN**). A *“qualitative” (coarse) target classification is therefore possible*, at least for situations with a sufficient signal to noise (S/N) ratio. Quantitative aspects are dealt with in [1].

## Acknowledgment

The members of the former EPFL/DeTeC team built the gantry and data acquisition electronics and thus made data acquisition and collection possible. Many colleagues at VUB-ETRO, in particular Valentin Enescu, Timofei Savelyev and Luc van Kempen, did play an important role in system setup and data acquisition. Joris Lochy carried out a “Werkkollege” which was instrumental in wrapping up the acquisition and analysis work. This work has been partially supported by the Swiss Office for Education and Science (OFES) within the EC IST EUDEM2 project ([www.eudem.info](http://www.eudem.info)).

## 12. References

- [1] C. Bruschini, L. van Kempen, and J. Lochy, “Metal Target Discrimination with a Commercial Two Frequency Sensor—Part II: Quantitative Aspects”, these proceedings.
- [2] C. Bruschini and H. Sahli, “Phase angle based EMI object discrimination and analysis of data from a commercial differential two frequency system”, in *SPIE Proceedings Vol. 4038*, pp. 1404-1419, Orlando, FLA, April 24-28, 2000.
- [3] C. Bruschini, “A Multidisciplinary Analysis of Frequency Domain Metal Detectors for Humanitarian Demining”, PhD Thesis, Vrije Universiteit Brussel (VUB, Belgium), Faculty of Applied Sciences, Brussels, Belgium, Sept. 2002, 230 pp. See <http://www.eudem.info/>
- [4] R. H. Chesney, Y. Das, J. E. McFee, and M. R. Ito, “Identification of Metallic Spheroids by Classification of Their Electromagnetic Induction Response”, *IEEE PAMI*, **6**(6), pp. 809-820, Nov. 1984.
- [5] P. Gao, *et al.*, “Enhanced Detection of Landmines using Broadband EMI”, in *SPIE Proceedings Vol. 3710*, Orlando, FLA, USA, April 1999, pp. 2-13.
- [6] P. Szyngiera, “A Method of Metal Object Identification by Electromagnetic Means”, in *Proc. MINE'99 (Mine Identification Novelties Euroconference)*, Florence, Italy, October 1-3, 1999, pp. 155-160. Available from <http://demining.jrc.it/aris/events/mine99/index.htm>.